IJR International Journal of Railway
Vol. 4, No. 2 / June 2011, pp. 34-41

The Korean Society for Railway

A Test Study on Interface Dynamics of Current Collection System in High Speed Trains

Jung Soo Kim† and Jae Hyun Han*

Abstract

Using a test run data, the dynamics of the interface between the catenary and pantograph constituting the current collection system in high-speed trains are investigated. The test run signals are analyzed to determine the dynamic parameters critical to the current collection performance. There are found to be frequency components of the pantograph motion that are dependent on train speed as well as components that are stationary such as the resonant mode of the panhead suspension in the pantograph. From contact force measurement using load cell, the mean contact force was found to be stable while the fluctuating component was found to be dependent on the range of the frequency of the pantograph motion taken into account. The finding implies that numerical investigations reported in the literature that are based on lumped element models of the catenary and/or pantograph provide accurate predictions on the mean value but are of limited use in estimating fluctuation of the contact force. It is concluded that simulation studies based on lumped-element models which do not incorporate panhead structural vibration modes is inaccurate at high train speeds.

Keywords **:** *Catenary, Current collection system, Dynamics, High speed train, Pantograph*

1. Introduction

The current collection system in high-speed train provides the required electrical power to the train. It is composed of the catenary and the pantograph that are in contact with each other. The catenary is an overhead slender structure composed of wires, repeating spans, and hangers. The pantograph is a device that acts as a conduit for delivering electrical power from the catenary to the train. During train operation, the pantograph and catenary must remain in physical contact at all times since the separation causes power loss and high temperature arcs at the interface between them. As the magnitude of the dynamic fluctuations tends to increase with increased train speed, ensuring proper contact at the catenary-pantograph interface has become a critical issue for high-speed trains.

The current collection system is fairly complex and different approaches have been taken to investigate its dynamics. Perhaps the most popular approach due to their ease and economy is the mathematical modeling and analysis of the catenary-pantograph dynamics. For instance, Park et al. (1999) performed numerical analyses of the catenary-pantograph motion based on finite difference schemes. Another line of investigation has been the characterization of the dynamics of the pantograph. Seering et al. (1991) constructed a nonlinear, lumped parameter model and compared the model predictions with experimental data. Park et al. (2003) performed the dynamic sensitivity analysis of a lumped parameter model of the prototype pantograph for high-speed train based on a new concept design involving reduced panhead mass (Han et al., 1998).

On the experimental side, investigations have utilized scale models. For instance, Farr et al. (1961), Willets and Edwards (1966) constructed dynamically equivalent laboratory scale models to study the effect of the design variables on the current collection behavior at low train speeds. Owing to scaling factors as high as 40:1, significant distortions were perhaps inevitable in their results. By conducting tests on a more realistically scaled model for high-speed trains, Manabe (1989) found that the perfor-

† Corresponding author: Department of Mechanical and System Design Engineering, Hongik University, Korea
E-mail: apolllo11@hanmail.net
* Department of Mechanical Engineering, Hongik University, Korea

mance of the caternary-pantograph system rapidly deteriorates with increasing train speed.

Because of difficulties in planning and implementing full-scale measurement as well as the difficulty of making modifications on the catenary-pantograph system for attaching appropriate sensors, relatively few investigations based on full-scale test runs have been reported. And a few that have been reported tended to be limited verifications of the overall system performance and not an in-depth dynamical analysis. (Seo et al., 2003) In the present study, the dynamic characteristics of the catenary-pantograph interface at full-scale are investigated based on signals acquired during an actual test run of a high-speed train.

The organization of the paper is as follows. In section 2, the measured signals at the catenary-pantograph interface are presented. In section 3, the signals are analyzed to elucidate critical dynamic parameters affecting the contact performance. In section 4, results on contact force measurement and analysis are presented. The results are summarized and conclusions are drawn in section 5.

2. Signal Measurement

The overall structure of the catenary-pantograph system is shown in Fig. 1. In the catenary, the electrical current is supplied to the train through the contact wire connected to the messenger wire by hangers. The hangers serve to transmit the weight of the contact wire onto the messenger wire. The span posts are used to provide vertical support for the catenary structure. There are devices called steady arms for providing lateral adjustment needed to protect the panhead from localized wear by moving the catenary sideways. Each span and hanger is given a predetermined sag, and as will be described later, the span spacing and the hanger spacing serve as important sources of the motion of the pantograph.

The pantograph is composed of three main segments and

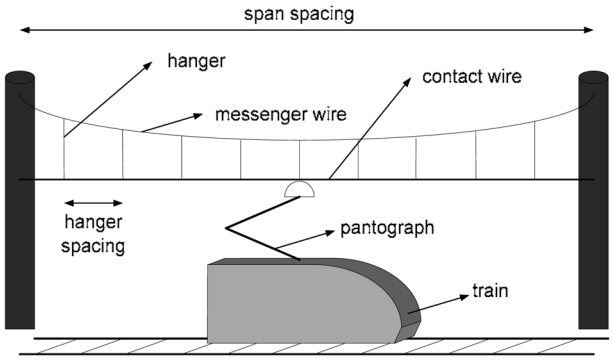

Fig. 1 Catenary-pantograph system

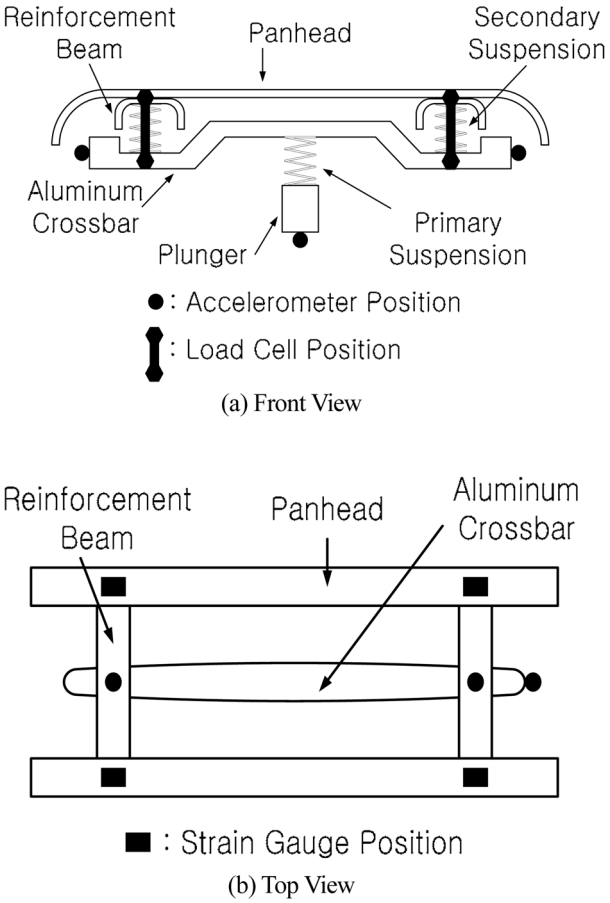

Fig. 2 Sensor locations

suspensions connecting them. The segment that comes in actual contact with the catenary is called the panhead. Fig. 2 illustrates the positions of the sensors attached to the pantograph assembly during the test run. To measure the movement of the panhead that comes in contact with the contact wire of the catenary, two accelerometers are attached on top of the reinforcement beams that connect the front and rear panheads and will heretofore be referred to as the panhead acceleration. Also, two load cells are placed between the panhead and aluminum crossbar below.

Fig. 3 shows the layout of the data acquisition system deployed to measure acceleration and load cell signals, while Fig. 4 shows the telemetry system for data acquisition.

Figs. 5 and 6 show the panhead acceleration and its root mean square (RMS) value as functions of the train speed, respectively. The rate of the increase in the acceleration is found to be roughly proportional to the square of the train speed. Thus, the catenary-pantograph interface is subject to ever greater fluctuating motion as the train gains speed.

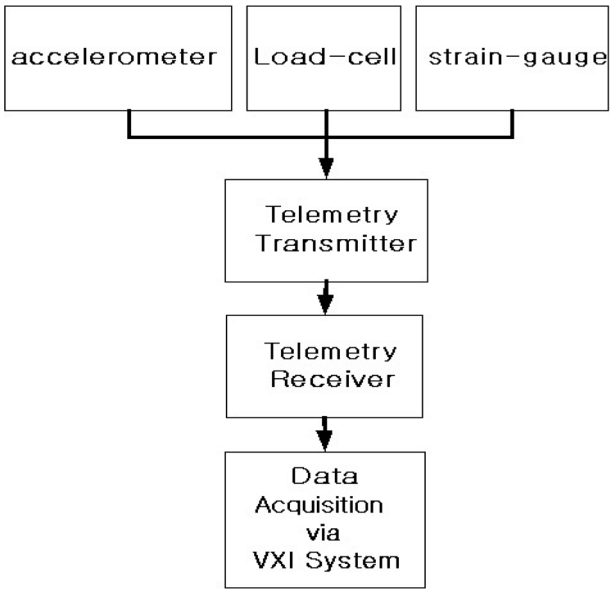

Fig. 3 Data acquisition system layout

(a) Transmitter

(b) Receiver and VXI Processing Unit

Fig. 4 Telemetry system

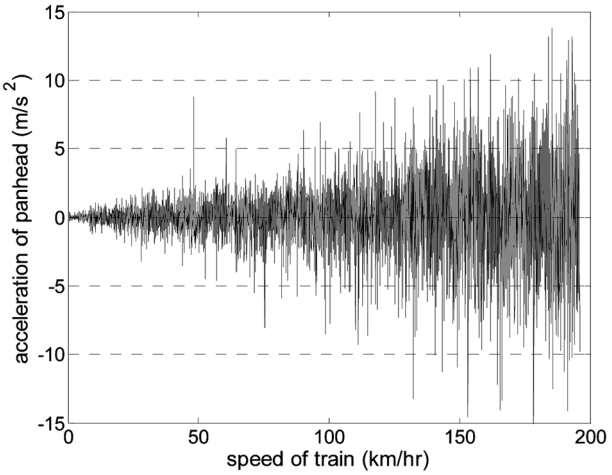

Fig. 5 Panhead acceleration vs. Train speed

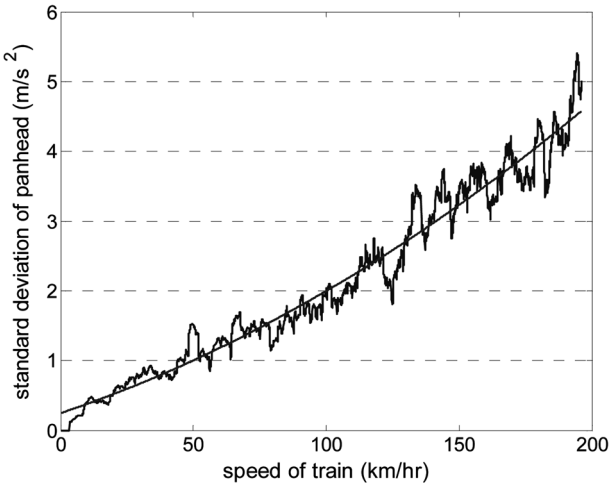

Fig. 6 RMS acceleration vs. Train speed

Fig. 7 depicts the load on panhead suspensions as a function of the train speed. The sinusoidal profile evident in a single load cell signal is due to the stagger of the catenary. The stagger shown in Fig. 8 moves the point of contact left and right, delocalizing the point of contact and evenly spreading wear on the panhead. The load cell, since it is located at a certain distance away from the center of the panhead, reaches a local maximum when the point of contact staggers closest to it and a local minimum when the point staggers farthest from it. The period of this sinusoid corresponds to the time required for the train to traverse a span. The period should diminish as the train speed increases, in direct proportion to the train speed as shown in Fig. 9. The inverse of the period is the span-passing frequency.

Figs. 10 and 11 show the mean and the standard deviation of the combined panhead load cell value, respec-

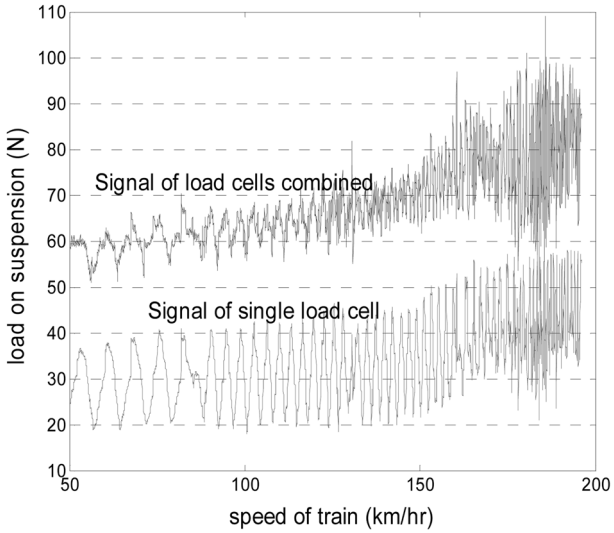

Fig. 7 Load vs. Train speed

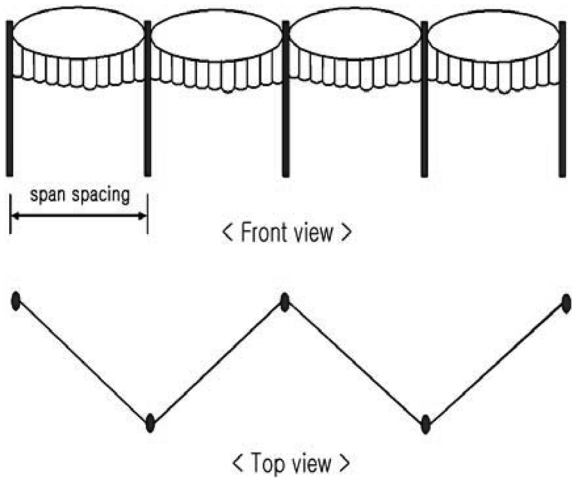

Fig. 8 Stagger in the catenary

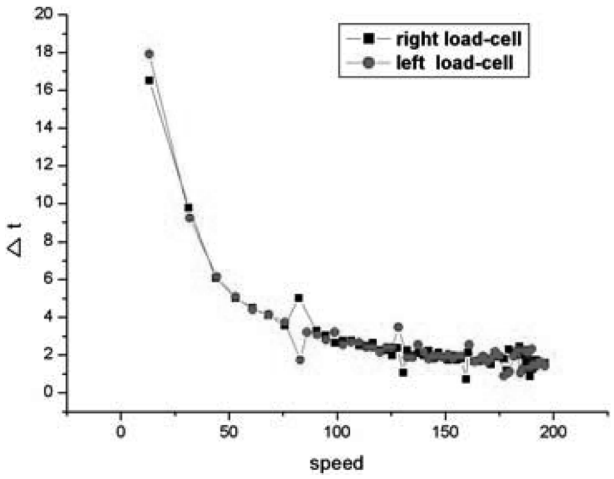

Fig. 9 Load cell period vs. Train speed

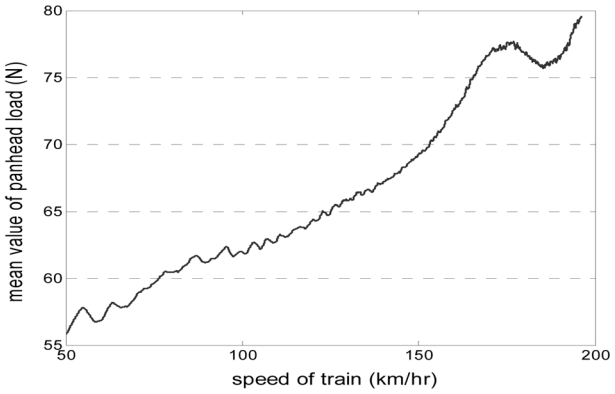

Fig. 10 Mean value of suspension load

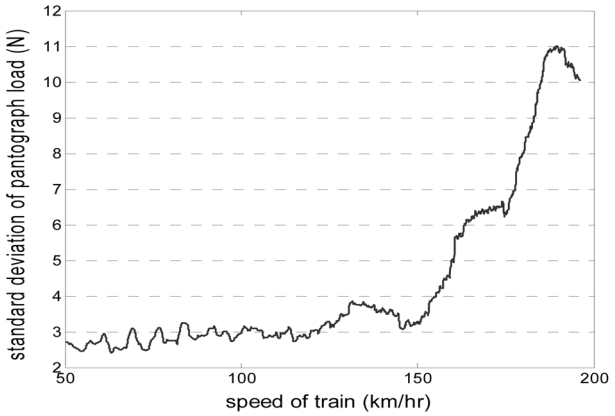

Fig. 11 Fluctuation in suspension load

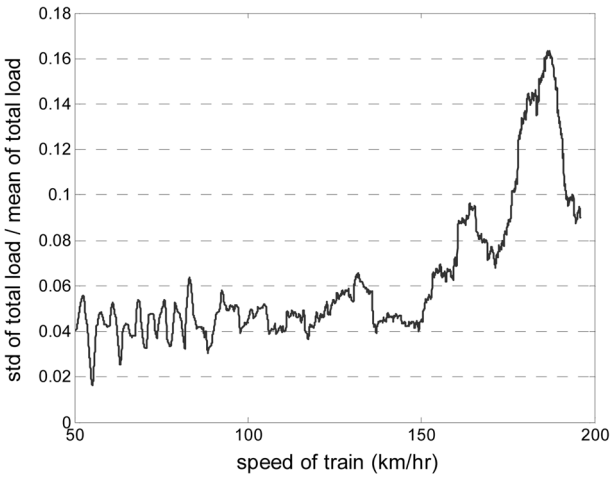

Fig. 12 Fluctuation ratio

tively. While the mean value shows steady increase with the train speed, the standard deviation shows much steeper increase from 150 km/hr onward.

Fig. 12 shows the standard deviation of the load divided by the mean of the same load. The fluctuation ratio

remains low until 150 km/hr then rapidly increases. The increase in this ratio refers to relatively greater fluctuating components of the contact load which is not desirable from the stable interface dynamics point of view.

3. Signal Analysis

Fig. 13 shows the panhead acceleration at the train speed of 196 km/hr in the frequency domain. Several major frequency components can be observed in Fig. 13(a). The first peak at 1.4 Hz is the span-passing frequency. The train speed is 196 km/hr and from the load cell data, the length of the span is found to be 40 m. The time elapsed for the train to traverse the span length is therefore 0.73 seconds. Taking the inverse, the frequency is found to be 1.4 Hz. The higher harmonics of the span-passing frequency are also observed. These harmonics have the frequency of two and three times the span-passing frequency and appear intermittently throughout the run. Since this component arises from the interaction between the pantograph and the catenary as the pantograph traverses along the prescribed sag in the contact wire, it is dependent on the train speed. The span-passing frequency shifts in direct proportion to the increase in the train speed.

The hanger-passing frequency component, i.e., the frequency corresponding to the train traversing the hanger length which is 1/9 of the span length - there are nine hangers per span - is also speed dependent. However, this component is not pronounced in the figure.

A large peak observed at 8.5 Hz is due to the fundamental resonant mode of the panhead assembly. Unlike the span-passing frequency component, this component is independent of the train speed. A simulation run based on finite difference modeling of the identical catenary and pantograph has predicted that the resonant mode at 8.5 Hz will be an important part of the pantograph motion. (Park et al., 1999).

For illustration purpose, higher frequency components due to the structural vibration of the panhead are shown in Fig. 13(b). As expected, these components are independent of the train speed.

To illustrate the speed-dependent nature of the acceleration signal of Fig. 13(a), Fig. 14 compares the frequency components of the panhead at two different train speeds. The speed for the upper graph is 148 km/hr and the lower is 193 km/hr. Since the train speeds of the two graphs differ, the speed dependent span-passing component must also differ by the same amount. The first peak for the upper graph is placed at 1.09 Hz and the lower graph is at 1.33 Hz, providing a direct evidence that the first peak shifts to a higher frequency as the train speed increases. On the other hand, the frequency of the speed-indepen-

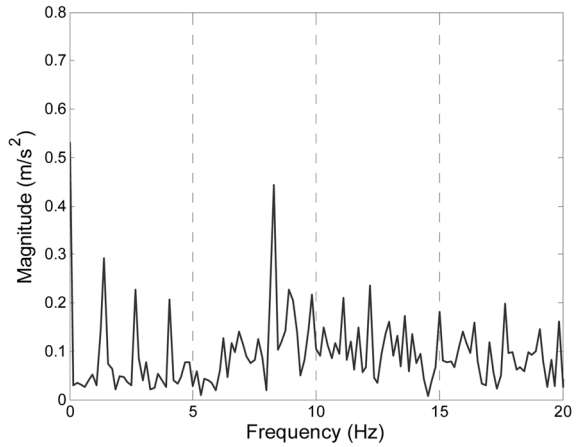

(a) Panhead Motion

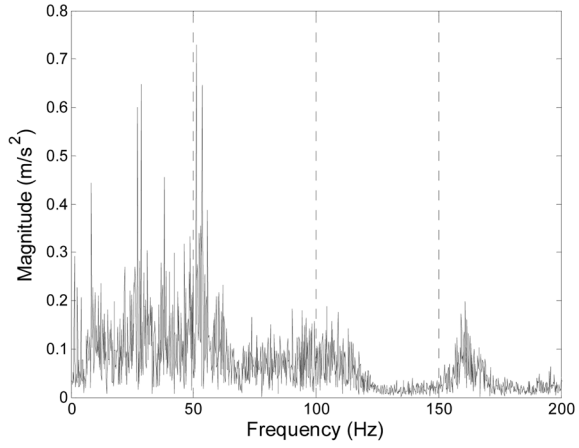

(b) Structural Vibration

Fig. 13 Panhead motion in frequency domain

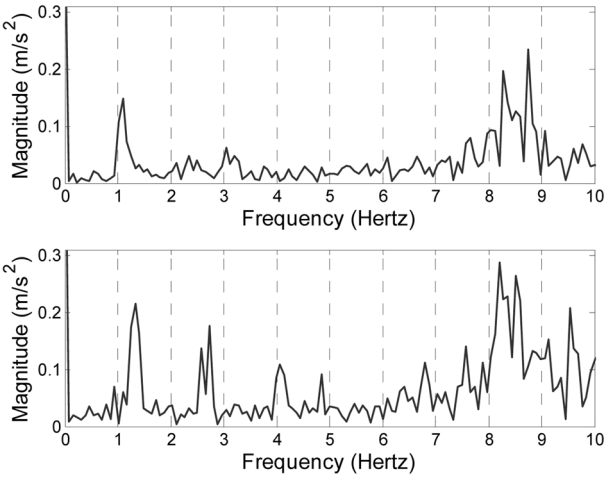

Fig. 14 Shifting of span-passing frequency

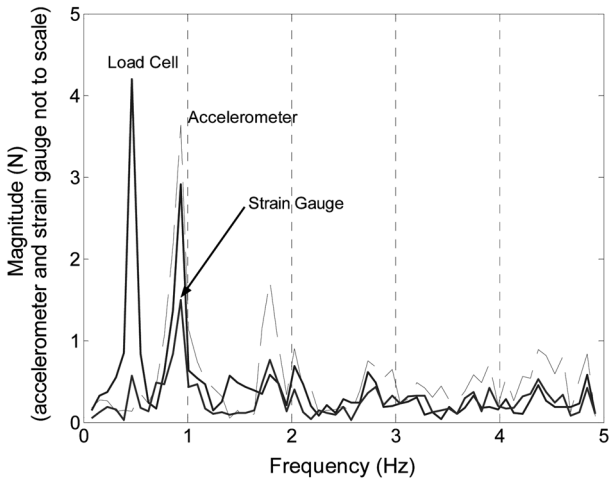

Fig. 15 Frequency components of sensors

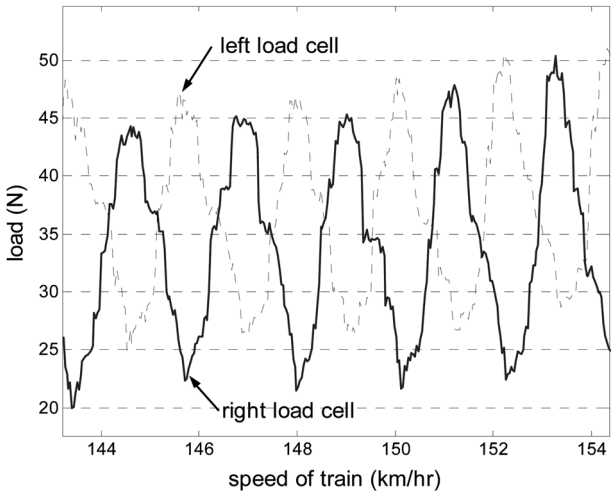

Fig. 16 Rolling motion of panhead

dent 8.5 Hz component remains stationary irrespective of the train speed.

Fig. 15 compares the frequency response of the load cell together with the accelerometer and strain gauge signals. The first peak of the accelerometer signal, representing the span-passing component, coincides with the second peak of the load cell signal and the first peak of the strain gauge signal.

The first peak observed in the load cell signal is one-half of the span-passing frequency and is a result of the rolling motion caused by the stagger induced in the catenary by the steady arms. The load cell must traverse two spans to complete a rolling motion. The rolling motion exists, as illustrated by Fig. 16, but an undesirable pitching motion that may adversely affect the performance of the current collection system is not pronounced due to the perfect symmetry of the pantograph design in the front-rear direction.

4. Contact Force Analysis

The contact force existing at the interface between the catenary and the panhead is an important indicator of the performance of the current collection system. If the contact force is too low, increased separation will result in excessive arcs and lead to the erosion of localized areas of the panhead. On the other hand, if the contact force is too high, the panhead will maintain contact with the catenary but at the cost of increased wear of the panhead. Therefore, the contact force needs to be maintained within a specified range.

A direct measurement of the contact force would require sensors to be placed at the interface between the contact wire and the panhead. However, this is not feasible due to a relative motion as well as high voltage current passing between them. A method for getting around this problem is to place the load cells below the panhead. But by doing so, the inertia force due to the movement of the panhead must be considered, i.e., the measured load cell signals need to be compensated by properly accounting for the acceleration of the panhead mass. The contact force can be represented as a sum of the load measured by the load cells attached to the bottom of the panhead, and the inertia force due to the panhead acceleration.

$$F_{contact} = F_{load\ cell} + F_{panhead\ inertia} \tag{1}$$

A methodology for calculating the inertia force from the accelerometer signals is now described. In our calculation of the inertia force, we will first consider only the rigid body motion of the panhead which enables us to ignore i.e., to filter out high frequency components of the accelerometer signal originating from the structural vibration of the panhead. Since the 8.5 Hz component represents the major resonant mode of the panhead assembly in which the overall panhead motion takes place over the suspension, i.e., since it is the major frequency component that is below the structural vibration frequencies, a 12 Hz low-pass filtering is deemed adequate to ensure that all structural vibration components are filtered out. With the rigid body assumption, the inertia force can be computed as a simple product of the panhead acceleration and the panhead mass. Equation (1) takes on a simple form given by

$$F_{contact} = F_{load\ cell} + m_{panhead} \cdot a_{accelerometer} \tag{2}$$

This approach is in line with most of the analytical and numerical studies that are based on lumped parameter models of the pantograph in which the panhead is treated as a lumped mass element.

However, the panhead can more accurately be modeled as an elastic structure rather than a rigid body, and the

inertia force contribution of the structural vibration of the panhead cannot be neglected if greater accuracy is desired. We therefore investigate the effect of including higher frequency components of the accelerometer signal in the inertia force estimation. By increasing the cutoff frequency, the rigid body restriction is alleviated as at least some of the structural vibration components of the panhead motion shown in Fig. 13(b) begin to be included in the inertia calculation.

Strictly speaking, the present calculation of the panhead inertia force as a simple product of the panhead mass and the accelerometer signal with a 20 Hz or a 30 Hz filtering applied to it is at best a rough estimate. The structural vibration of the panhead involves a relative motion between different locations within the panhead, and the many more acceleration measurements at selected locations within the panhead structure is probably needed to accurately determine the structural vibration contribution to the panhead inertia force. As a practical matter, the inertia force can be calculated as a weighted sum of all the accelerometer signals collected at selected locations within the panhead, with the weighting factor for each signal suitably determined. For greater accuracy, greater number of such acceleration signals with suitably determined weighting factors will be required. In the present study, just two accelerometer signals are used with an equal weighting factor of 1/2 for each. Equation (2) is still applicable but with the panhead acceleration term expanded to include the higher frequency contributions due to the structural vibration. The contact force calculated according to equation (2) is expected to provide a satisfactory qualitative trend, if not accurate quantitative predictions.

Fig. 17 divides the predicted contact forces into the mean and fluctuating parts for different cutoff frequencies deployed. While the mean value of the predicted contact force noticeably increases with the train speed, the influence of the cutoff frequency on the mean is found to be rather slight. In contrast, the fluctuation of the contact force from the mean as measured by the standard deviation is significantly affected by the cutoff frequency as shown at the bottom of Fig. 17. At the top train speed of 200 km/hr, the mean contact force is found to be around 85 N for all three cutoff frequencies while almost two-fold increase in the standard deviation from 11 N to 20 N is observed between the 12 Hz and 30 Hz cutoff frequency.

An important implication of the present finding is that analytical or numerical investigations based on multi-degree-of-freedom discretized models of the catenary and/or pantograph could provide accurate predictions on the mean value of the contact force but may not fully account for fluctuations influenced by the high-frequency structural vibration components. Since the ratio of the fluctuating portion to the mean value portion in the contact force increases with increasing train speed, the predictive capacity of the investigations based on numerical simulations utilizing lumped parameter models of the pantograph diminishes as train speed increases.

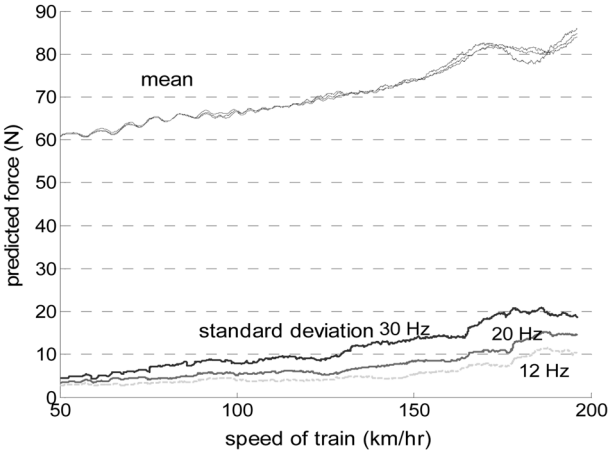

Fig. 17 Mean and fluctuation of contact force

5. Conclusions

The interface dynamics of the current collection system in high-speed trains are evaluated by examining signals collected during a test run. The overall acceleration of the pantograph at the interface increases to the square of the train speed. It also shows the presence of a rolling mode but no undesirable pitching mode.

The frequency domain analysis has isolated major frequency components of the pantograph motion such as the span-passing, hanger-passing, and the resonant mode of the panhead suspension. They can be divided into components that shift in direct proportion to the train speed such as the span-passing modes and into stationary components such as the 8.5 Hz panhead resonant mode and a multitude of structural vibration modes.

The contact force can be calculated by taking a sum of the load cell signals and the panhead inertia force. The inertia force calculation uses the accelerometer signal low-pass filtered with a suitable cutoff frequency. The mean value of the contact force does not vary much as the cutoff frequency is varied from 12 Hz to 30 Hz, but the fluctuation about the mean increases as the cutoff frequency is increased. Thus, the choice of a cutoff frequency will significantly influence the predicted fluctuation of the contact force about the mean value but not the mean value itself. It can be surmised that multi-degree-of-freedom dis-

cretized models of the catenary and/or pantograph that do not account for the structural vibration of the panhead may not be adequate in predicting contact force in high train speeds.

Acknowledgment

This work was supported by 2008 Hongik University Research Fund.

References

1. Farr, D. S., Hall, H. C. and William, A. L. (1961). "A dynamic model for studying the behaviour of the overhead equipment used in electric railway traction," Proc. IEE, No. 3530U, pp. 421-434.
2. Han, H. S., Kyung, J. H., Song, D. H. and Bae, J. C. (1998). "Concept design of the pantograph for high speed trains," Proc. KSR, pp. 337-344.
3. Manabe, K. (1989). "High speed contact performance of a catenary-pantograph system," JSME Int. J., Vol. 32, No. 2, pp. 200-205.
4. Park, S. H., Kim, J. S., Hur, S., Kyung, J. H. and Song, D. H. (1999). "On dynamic characteristics of TGV-K pantograph-catenary system," Proc. KSR, pp. 176-184.
5. Park, T. J., Han, C. S. and Jang, J. H. (2003). "Dynamic sensitivity analysis for the pantograph of a high-speed rail vehicle," J. Sound and Vibration, Vol. 266, pp. 235-260.
6. Seering, W., Armbruster, K., Vesely, C. and Wormley, D. (1991). "Experimental and analytical study of pantograph dynamics," J. Dynamic Systems, Measurement and Control, Vol. 113, pp. 242-247.
7. Seo, S. I., Park, C. S., Cho, Y. H., Choi, K. Y., Mok, J. Y. and Kang, B. B. (2003). "Test and evaluation of the pantograph for korean high speed train," KRRI Report
8. Willetts, T. A. and Edwards, D. R. (1966). "Dynamic-model studies of overhead equipment for electric railway traction," Proc. IEE., Vol. 133, No. 4, pp. 690-696.

Received(June 10, 2011), Accepted(June 25, 2011)